

Direct eicosanoid profiling of the hypoxic lung by comprehensive analysis via capillary liquid chromatography with dual online photodiode-array and tandem mass-spectrometric detection

Ladislau Kiss · Yasmin Röder · Jens Bier ·
Norbert Weissmann · Werner Seeger ·
Friedrich Grimminger

Received: 15 June 2007 / Revised: 12 October 2007 / Accepted: 23 October 2007 / Published online: 14 December 2007
© Springer-Verlag 2007

Abstract Eicosanoids are arachidonic acid-derived mediators, with partly contradictory, incompletely elucidated actions. Thus, epoxyeicosatrienoic acids (EETs) are controversially discussed as putative vasodilative endothelium-derived hyperpolarizing factors in the cardiovascular compartment but reported as vasoconstrictors in the lung. Inconsistent findings concerning eicosanoid physiology may be because previous methods were lacking sensitivity, identification reliability, and/or have focused on special eicosanoid groups only, ignoring the overall mediator context, and thus limiting the correlation accuracy between autacoid formation and bioactivity profile. Therefore, we developed an approach which enables the simultaneous assessment of 44 eicosanoids, including all representatives of the arachidonic acid cascade, i.e., cytochrome P450, lipoxygenase, cyclooxygenase products, and free isoprostanes as *in vivo* markers of oxidative stress, in one 50-minute chromatographic run. The approach combines (i) source-specific sample extraction, (ii) rugged isocratic and high-sensitivity capillary liquid-chromatographic separation, and (iii) reliable dual online photodiode-array and electrospray ionization tandem mass-spectrometric identification and quantitation. High sensitivity with limits of quantification in the femtogram range was

achieved by use of capillary columns with typical high peak efficiency, due to small inner diameters, and virtually complete substance transfer to the mass spectrometer, due to flow rates in the low microliter range, instead of large inner diameter columns with low chromatographic signal and only partial analyte transfer employed by previous methods. This expeditious, global and sensitive technique provides the prerequisite for new, accurate insights regarding the physiology of specific mediators, for example EETs, in the context of all relevant vasoactive autacoids under varying conditions of oxidative stress by direct comparison of all eicosanoid generation profiles. Indeed, application of comprehensive “eicoprofiling” to hypoxically ventilated rabbit lungs revealed at a glance the enhanced biosynthesis of free EETs in the overall mediator generation context, thus suggesting their hypothetical contribution to hypoxic pulmonary vasoconstriction.

Keywords Eicosanoid profiling · Isocratic capillary liquid chromatography · Photodiode-array detection · Tandem mass-spectrometric detection · Multiple reaction monitoring · Extracted ion chromatogram

Abbreviations

SPE	Solid-phase extraction
CapLC	Capillary liquid chromatography
HPLC	High-performance liquid chromatography
RT	Retention time
RRI	Relative retention index
PDA(D)	Photodiode array (detector/detection)
L	Length
i.d.	Inner diameter
UV	Ultraviolet

Electronic supplementary material The online version of this article (doi:10.1007/s00216-007-1718-9) contains supplementary material, which is available to authorized users.

L. Kiss (✉) · Y. Röder · J. Bier · N. Weissmann · W. Seeger ·
F. Grimminger
Biochemie Med. II, University of Giessen Lung Center (UGLC),
Department of Internal Medicine, Justus Liebig University,
Paul Meimberg Str. 5,
35392 Giessen, Germany
e-mail: ladislau.kiss@innere.med.uni-giessen.de

MS	Mass spectrum/spectrometry/spectrometric
ESI	Electrospray ionization
EIC	Extracted ion chromatogram
MRM	Multiple reaction monitoring
ICC	Ion charge control
DI	Direct infusion
LOQ	Limit of quantification
S/N ratio	Signal-to-noise ratio
CYP	Cytochrome P450
LOX	Lipoxygenase
COX	Cyclooxygenase
AA	Arachidonic acid
LT	Leukotriene
LX	Lipoxin
HETE	Hydroxyeicosatetraenoic acid
12-HHT	12-Hydroxyheptadecatrienoic acid
EET	Epoxyeicosatrienoic acid
DHET	Dihydroxyeicosatrienoic acid
DiHETE	Dihydroxyeicosatetraenoic acid
PG	Prostaglandin
TX	Thromboxane
iPT	Isoprostane
ROS	Reactive oxygen species
SDA	Stearidonic acid
BHT	Butylated hydroxytoluene
IS	Internal standard
ODS	Octadecyl silyl
EDHF	Endothelium-derived hyperpolarizing factor
HPV	Hypoxic pulmonary vasoconstriction
Δ PAP	Pulmonary arterial pressure rise
KHB	Krebs–Henseleit buffer
FA	Formic acid
DEA	Diethylamine
TEA	Triethylamine
BSA	Bovine serum albumin

Introduction

Eicosanoids are potent lipid mediators derived from arachidonic acid (AA), an essential component of cellular membrane lipids, via the cytochrome P450 (CYP), lipoxygenase (LOX), and cyclooxygenase (COX) pathways but also non-enzymatically by interaction with reactive oxygen species (ROS) [1–4] (Fig. 1). The different autacoids/autacoid groups, like the CYP-mediated epoxyeicosatrienoic acids (EETs) and 20-hydroxyeicosatetraenoic acid (20-HETE), the soluble epoxide hydrolase (sEH)-mediated dihydroxyeicosatrienoic acids (DHETs), the LOX-mediated leukotrienes (LTs) and lipoxins (LXs), the COX-mediated prostaglandins (PGs), thromboxanes (TXs), and 12-heptadecatrienoic acid (12-HHT), the *cis-trans* conjugated hydroxyeicosatetraenoic acids (HETEs)

mediated by CYP, LOX, or COX, and the isoprostanes (iPTs) generated by the impact of ROS on AA and therefore used as reliable in-vivo indicators of ROS levels and oxidative stress, have a broad array of biological functions, from proinflammatory and vasoconstrictive to anti-inflammatory and vasodilative [1–3, 5, 6].

Among all eicosanoids, the CYP-derived 20-HETE and EETs, and the sEH-derived DHETs with reportedly contradictory vasoregulative functions are of particular interest. These mediators are described as both vasodilators and vasoconstrictors acting by themselves, via metabolism by COX, or by inducing the expression of COX and thus the enhanced production of prostanoids [6–9]. Although EETs/DHETs were proposed over a decade ago as chemical correlates of the vasodilative endothelium-derived hyperpolarizing factor (EDHF) in the cardiovascular compartment, and discussed since then [10–14], there still is no agreement about the nature of EDHF despite sustained efforts concerning characterization and identification. In the lung, in contrast to the other compartments, the role of EETs is poorly investigated, but first reports describe them as both vasoconstrictors and vasodilators [6, 7]. Interestingly, 20-HETE is a vasodilator in the lung but a vasoconstrictor in all other compartments and antagonizes EDHF-mediated relaxation [6, 9]. Intriguingly, CYP enzymes may control vascular homeostasis by simultaneous production of EETs, 20-HETE, and ROS [15]. ROS may be involved in vasoregulation directly [16] or by generating iPTs, considered as not just markers of oxidative stress but also as vasoconstrictors [3] and even as candidates for EDHF [17].

This brief synopsis suggests that comprehension of eicosanoid physiology is quite difficult when analyzing only some autacoids without considering all the other relevant mediators and the actual oxidative stress status. Thus, the question arises: What is the *relative*, i.e., *actual* contribution of 20-HETE, EETs, and DHETs in the context of *all* vasoactive representatives of the AA cascade and the iPTs to the observed physiological effect? To answer this question, a global profiling technique is required to enable direct comparison of *all* eicosanoid generation profiles as a prerequisite for comprehensive and differentiated understanding of the physiological role of 20-HETE, EETs, and DHETs in the overall mediator context, including possible interrelations with other autacoids, under conditions of variable ROS concentrations.

The aim of this work was to provide a set of bioanalytical information suitable for elaboration, as a basis for further investigations, of a first solid hypothesis regarding the role of free (i.e., not esterified into cellular membrane phospholipids) EETs, DHETs, and 20-HETE in epithelial/endothelial homeostasis in general and their contribution to EDHF-mediated responses and to hypoxic pulmonary vasoconstriction (HPV) in particular by use of a comprehensive method

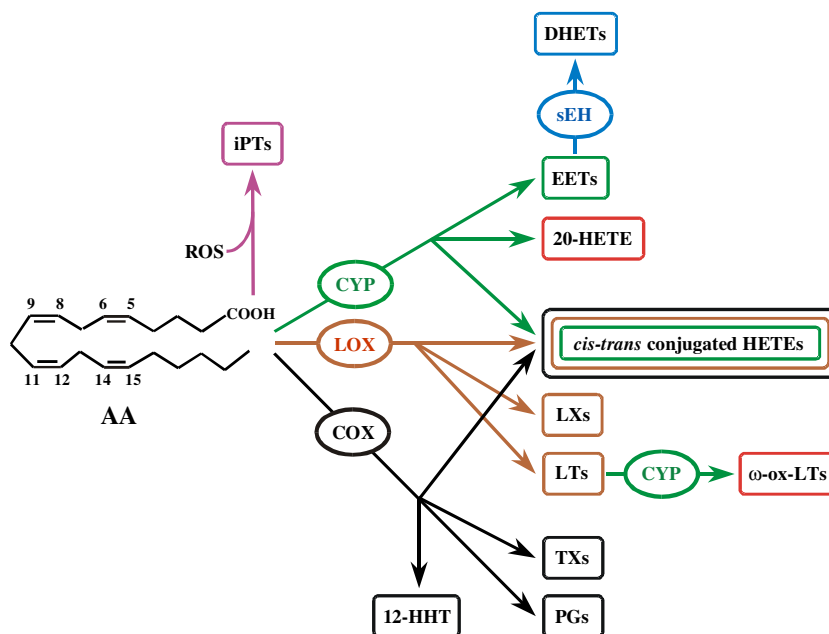


Fig. 1 Eicosanoid formation via the three main pathways of the AA cascade—CYP, LOX, and COX—and non-enzymatically by interaction of AA with ROS. AA = arachidonic acid; CYP = cytochrome P450; LOX = lipoxygenase; COX = cyclooxygenase; sEH = soluble epoxide hydrolase; ROS = reactive oxygen species; EETs = epoxyeicosatrienoic acids (42=14,15-EET, 43=11,12-EET, 44=8,9-EET, 45=5,6-EET); DHETs = dihydroxyeicosatrienoic acids (36=14,15-DHET, 37=11,12-DHET, 38=8,9-DHET, 40=5,6-DHET, 41=5,6-DHET δ lactone); 39=20-HETE = ω -oxygenase-mediated 20-hydroxyeicosatetraenoic acid; HETEs = hydroxyeicosatetraenoic acids (16=15-HETE, 17=11-HETE, 18=8-HETE, 19=12-HETE, 20=9-HETE, 21=5-HETE); LXs = lipoxins

(2=LXA₄, 1=LXB₄); LTs = leukotrienes (11=LTB₄, 7=LTC₄, 6=LTD₄, 8=LTE₄); ω -ox-LTs = ω -oxygenase-mediated LT metabolites (5=20-HO-LTB₄, 4=20-COOH-LTB₄); TXs = thromboxanes (TXA₂, 29=TXB₂, 26=2,3-dinor-TXB₂, 24=11-dehydro-TXB₂); PGs = prostaglandins (PGI₂, 28=6-keto-PGF_{1 α} , 27=2,3-dinor-6-keto-PGF_{1 α} , 23=6-keto-PGE₁, 33=PGE₂, 22 = 19(*R*)-hydroxy-PGE₂, 34=PGD₂, 35=PGJ₂, 14= Δ ¹²-PGJ₂, 3=15-deoxy- Δ ^{12,14}-PGJ₂, 31=PGF_{2 α} , 32=13,14-dihydro-15-keto-PGF_{2 α}); 15=12-HHT = 12-hydroxyheptadecatrienoic acid; iPTs = isoprostanes (30=8-*iso*-PGF_{2 α} , 25=2,3-dinor-8-*iso*-PGF_{2 α}). Eicosanoid numbering is the same as in Fig. 2

which enables accurate correlation between generation and bioactivity profiles of all the biologically relevant eicosanoids at a glance. High-performance liquid chromatographic (HPLC) separation followed by online spectrophotometric and/or gentle electrospray ionization mass-spectrometric (MS) detection is best suited for the analysis of a broad array of these unstable compounds [18–23]. The disadvantages of other techniques, for example gas chromatography–MS or HPLC with fluorescence detection reside in incomplete separation at high temperatures of the thermolabile autacoids or high background interference, respectively, and their need for sample derivatization [24, 25]. As free eicosanoids generally occur in biological sources at very low concentrations, the above mentioned aim can be achieved only by use of a method which is not merely comprehensive but also highly sensitive. Quantitative sensitivity can be improved dramatically by the use of capillary columns with small inner diameters (i.d. <0.5 mm) instead of large i.d. columns (microbore, narrowbore, or conventional analytical columns with i.d.=1–4.6 mm), employed by previous methods, because of two major sensitivity-increasing factors:

1. peak efficiency, i.e., chromatographic signal intensity, is inversely proportional to column i.d. and thus very

much higher for capillary columns than for large-i.d. columns, and

2. substance transfer from the capillary column to the mass spectrometer is virtually complete, because of the typically very low column effluent flow rates in the low microliter range in contrast with only partial analyte transfer because of the high flow rates typical of large-i.d. columns.

We therefore developed a technique combining:

1. source-specific sample extraction,
2. rugged isocratic and high-sensitivity capillary liquid chromatographic (CapLC) separation, and
3. reliable dual online photodiode array (PDAD) and electrospray ionization (ESI) tandem mass-spectrometric (MS²) detection in the negative-ion mode employing an ion-trap mass spectrometer for simultaneous identification and quantitation of all relevant CYP, sEH, LOX, and COX-derived eicosanoids (EETs, DHETs, 20-HETE, LTs, LXs, DiHETEs, PGs, TXs, 12-HHT, HETEs) and free iPTs within one chromatographic run.

Application of this CapLC–PDAD–ESI–MS² method to hypoxic lung homogenate demonstrated its robustness,

reliability, and high sensitivity in comprehensive “eico-profiling” down to the femtogram range.

Experimental

Standards, chemicals, reagents, and solvents

The epoxyeicosatrienoic acids 14,15-EET, 11,12-EET, 8,9-EET, and 5,6-EET, and the dihydroxyeicosatrienoic acids 14,15-DHET, 11,12-DHET, 8,9-DHET, 5,6-DHET, and 5,6-DHET δ -lactone were supplied by Cascade Biochem (Reading, UK), Cayman Chemical (Ann Arbor, MI, USA), and Biomol (Hamburg, Germany). 12-HHT, 20-HETE, the hydroxyeicosatetraenoic acids 15-HETE, 11-HETE, 8-HETE, 12-HETE, 9-HETE, and 5-HETE, the leukotrienes 20-COOH-LTB₄, 20-HO-LTB₄, LTC₄, LTE₄, 6t-LTB₄, 6t,12e-LTB₄, LTB₄, and LTD₄, the lipoxins LXA₄ and LXB₄, the dihydroxyeicosatetraenoic acids 5(S),6(R)-DiHETE and 5(S),6(S)-DiHETE, and the non-deuterated internal standard (IS) prostaglandin B₁ (IS = PGB₁) were purchased from Biomol and Cayman. The prostaglandins 6-keto-PGF_{1 α} , 6-keto-PGE₁, 2,3-dinor-6-keto-PGF_{1 α} , PGD₂, PGJ₂, $\Delta^{12,14}$ -PGJ₂, 15-deoxy- $\Delta^{12,14}$ -PGJ₂, PGE₂, 19(R)-hydroxy-PGE₂, PGF_{2 α} , and 13,14-dihydro-15-keto-PGF_{2 α} , the isoprostanes 8-*iso*-PGF_{2 α} and 2,3-dinor-8-*iso*-PGF_{2 α} , the thromboxanes TXB₂, 11-dehydro-TXB₂, and 2,3-dinor-TXB₂, and stearidonic acid (SDA) were obtained from Cayman. The deuterated internal standards [²H₈]14,15-EET, [²H₈]11,12-EET, [²H₈]8,9-EET, [²H₈]5,6-EET-Me, [²H₈]15S-HETE, [²H₃]LTE₄, and [²H₃]2,3-dinor-6-keto-PGF_{1 α} , were purchased from Biomol. [²H₆]20-HETE, [²H₈]5S-HETE, [²H₈]12S-HETE, [²H₄]6-keto-PGF_{1 α} , [²H₄]PGD₂, [²H₄]15-deoxy- $\Delta^{12,14}$ -PGJ₂, [²H₄]PGE₂, [²H₄]PGF_{2 α} , [²H₄]8-*iso*-PGF_{2 α} , [²H₄]TXB₂, and [²H₄]11-dehydro-TXB₂ were obtained from Cayman, and [²H₄]LTB₄ was obtained from both Biomol and Cayman.

Butylated hydroxytoluene (BHT), triethylamine (TEA), and diethylamine (DEA) were obtained from Sigma (Munich, Germany). Ethylenediaminetetraacetic acid disodium salt dihydrate (EDTA Na₂·2H₂O), tetrasodium salt tetrahydrate (EDTA Na₄·4H₂O), and formic acid (FA) were purchased from E. Merck (Darmstadt, Germany). Bovine serum albumin (BSA) and Coomassie Brilliant Blue G-250 dye reagent were from Bio-Rad Laboratories (Munich, Germany).

Krebs–Henseleit-buffer supplemented with 5% hydroxyethyl starch (KHB) was obtained from Serag Wiessner (Naila, Germany). Water was purified with a Milli-Q Synthesis A10 system (Millipore, Eschborn, Germany). Methanol was from Burdick and Jackson (Muskegon, MI, USA), acetonitrile was purchased from J. T. Baker (Deventer, Netherlands), isopropanol was obtained from Fluka (Buchs,

Switzerland), and ethanol was from Merck. Table 1 shows the solvent mixtures used for solid-phase extraction (SPE).

SPE and CapLC–PDAD–ESI–MS² procedures and equipment

Eicosanoids were extracted from lungs by SPE and subjected to CapLC–PDAD–ESI–MS². Oxidative loss was prevented by addition of the antioxidant BHT from the very beginning of sample extraction, prior to any manipulation and throughout the whole analytical procedure.

SPE

Optimal purification and concentration of eicosanoids was achieved by an extraction procedure specifically developed for rabbit lung homogenate. Lungs were subjected immediately to homogenization and extraction or stored at –85°C for up to 24 h until further processing. For assessment of recoveries and for quality control, 0.5-g samples of biological matrix (homogenate from blood-free rinsed lungs) and 0.5 mL KHB alone were spiked with known amounts of eicosanoid standards, constant amounts of internal standards (PGB₁ and/or deuterated eicosanoids), SDA, and BHT. Genuine samples were processed in the same manner, except for supplementation with eicosanoid standards. In brief, 0.5 g tissue from hypoxic or normoxic rabbit lungs was supplemented with 50 μ L 15 mmol L^{–1} BHT in methanol, 50 μ L FA, 5 μ L of solution E (Table 1), internal standards, and SDA, and subjected to mechanical homogenization in a chilled 2-mL borosilicate glass tube for 10 min at 1,500 rpm employing a Potter S homogenizer with PTFE plunger mounted on a stainless steel shaft, all from Sartorius (Göttingen, Germany). The homogenate samples were diluted with 0.2 mL KHB. Aliquots thereof (0.5-mL) were supplemented with BHT (1.5 mmol L^{–1}, final concentration) and 0.7 mL solvent mixture F, then vortex mixed for 10 min and centrifuged for 30 min at 21250 g and 4°C. Prior to SPE, 0.6 mL supernatant was diluted with 4.4 mL of KHB and applied to the conditioned extraction cartridges filled with end-capped octadecylsilyl (ODS) silica (Chromabond; C18ec, sorbent mass, 200 mg; reservoir volume, 3 mL) mounted in a Chromabond vacuum manifold, all from Macherey–Nagel (Düren, Germany), without vacuum suction. Elimination of interfering substances was achieved by two-step elution of the columns with solvent mixtures optimized for this purpose (Table 1 and [electronic supplementary material Table S1](#)). After the final elution step, the collected samples were dried gently under a stream of N₂ and subjected immediately to CapLC–PDAD–ESI–MS² analysis or stored at –85°C for up to 24 h until further processing. Throughout the whole sample-handling procedure, beginning with homogeniza-

Table 1 Composition (% v/v) of the solvent mixtures

Solvent / reagent	A	B	C	D	E	F
Water	89.97	86.26	5		1 ^a	
Methanol			95	20		
Ethanol						50
Acetonitrile				80		50
Isopropanol	10.0	12.90				
FA	0.03	0.18	0.002 ^b			
TEA		0.66				
EDTA a ₄ .4H ₂ O					12 ^c	
		pH 5.0 ^d	pH 4.5 ^d			

^a Volume (mL)

^b The composition of solvent mixture C (% composition in methanol and water) does not take into account the small volume of FA added

^c Mass (mg)

^d Apparent pH adjusted by addition of TEA or FA using a glass electrode

The pH of mixture A was not adjusted

tion and during the extraction process, all tissues, samples, solvents, and eluents were kept at low temperatures.

CapLC–PDAD–ESI–MS²

The CapLC–PDAD–ESI–MS² system used for eicosanoid analysis consisted of two main parts:

1. A 1100 Series capillary LC unit (Agilent Technologies Deutschland, Waldbronn, Germany) comprising a binary micro pump, a micro autosampler thermostatted at 4°C and equipped with an 8- μ L sample loop, and a photodiode-array detector (PDAD) with a nano flow cell (500 nL volume, 10 mm path length). ChemStation Rev. A.09.03 software was employed for device control, raw data acquisition, integration, spectral analysis, and processing.
2. An Esquire 3000+ ion trap mass spectrometer (Bruker Daltonik, Bremen, Germany) equipped with an ESI source was connected to the PDAD of the CapLC unit by means of a 75-cm length of a 25- μ m inner diameter (i.d.) fused silica tubing. The peak efficiency of the capillary column and thus overall quantitative sensitivity was improved by avoidance of dead volume in the fluidic system of the CapLC–PDAD–ESI–MS² set-up by use of 25 μ m instead of 50 μ m i.d. fused silica tubing, beginning with the injection valve of the micro autosampler. Instrument control and MS² data processing was performed with the Esquire v 5.1 (Bruker) software fully integrated with the ChemStation Rev. A.09.03 (Agilent) software.

The ion trap used had the capability to perform fragmentation beginning with MSⁿ stage 2 ($n=2$, MS²) through MSⁿ stage 11 ($n=11$, MS¹¹). In the present method we employed only MS² fragmentation. N₂ was used as nebulizing and

drying gas, and He was used as collision gas. The ESI source conditions nebulizing gas pressure, drying gas flow, and drying gas temperature were set to 11.0 psi, 6.0 L min⁻¹, and 300°C, respectively. The sampling, transfer, and focusing voltages (capillary, skimmer, octapoles, lens) were optimized individually for each analyte by parameter ramping during direct infusion (DI) of analyte standards using a syringe pump (Cole-Parmer Instrument Company, Vernon Hills, IL, USA) at a rate of 2.5 μ L min⁻¹ (1–5 ng analyte min⁻¹). The capillary voltage was set to 3600–3800 V. Isolation width and collision energy in terms of fragmentation amplitude were individually optimized for each compound and set to 0.7–1.5 Da and 0.48–0.78 V, respectively. Mass cutoff was set to 27% of the m/z value of the precursor molecular ion. In order to ensure optimal loading of the trap even under conditions of varying ion beam currents due to eluting LC peaks typical for online LC–MS² coupling, the accumulation time was automatically adjusted by the ion charge control (ICC) parameter of the instrument. As a result, not only were the quantitation sensitivity and accuracy of the ion trap considerably improved but also the dynamic range of the instrument was greatly extended.

Separation of autacoids was performed on capillary columns (250 mm \times 150 μ m = $L \times$ i.d. and 250 mm \times 300 μ m = $L \times$ i.d.) filled with a high-purity spherical polymer-coated silica gel stationary phase of extremely high carbon content (Grom-Sil 80 ODS-7 pH with 22% C18; particle size, 4 μ m; pore diameter, 80 Å) from Grom Analytik + HPLC (Rottenburg-Hailfingen, Germany). Prior to injection of 8- μ L aliquots into the CapLC–PDAD–ESI–MS² system, biological or quality control samples dried after SPE were redissolved in 20 μ L solvent mixture D containing 30 μ mol L⁻¹ BHT, vortex mixed, supplemented with 20 μ L water, vortex mixed again, sonicated, and centrifuged briefly. Alternatively, 20- μ L aliquots of non-extracted eicosanoid standard mixtures for calibration, freshly prepared prior to analysis from the stock solution by serial dilution with solvent mixture D (Table 1) containing 30 μ mol L⁻¹ BHT and constant amounts of IS and SDA as reference substance, were supplemented with 20 μ L water, vortex mixed, sonicated, and centrifuged. Thus, maximal mass sensitivity of capillary separation was achieved by large-volume injection (8 μ L instead of typical 0.2 μ L) employing “on-column focusing” [26, 27], i.e., enrichment of the analytes at the top of the capillary column before penetrating the column bed by keeping the solvent strength of the sample weaker than that of the mobile phase (i.e., by diluting all samples 1:1 with water prior to injection). This compression effect not only counteracts the classical band broadening effect but, in addition, enables a considerable gain in peak efficiency under large-volume injection conditions. As mobile phase a

mixture of water–acetonitrile–methanol–FA (130:240:80:0.22, v/v/v/v) was used (pH 4.30, adjusted with DEA). The desired selectivity for the separation of the protophilic peptido-LTs (LTC₄, LTD₄, LTE₄) could sensibly be chosen by up or down regulation of pH in steps of 0.01. Flow rate was 2.7 μL min⁻¹ (for i.d.=300 μm) or 0.95 μL min⁻¹ (for i.d.=150 μm) and column oven temperature was 33°C. The eluting compounds were subjected to dual online spectrophotometric and tandem mass-spectrometric analysis by employing the consecutively interfaced PDAD and ion trap. The PDAD provided full UV spectra (190 to 400 nm) of eluting analytes, enabled the definition of up to five detection wavelengths, and allowed checking for peak purity and subtraction of possible coeluting material. The ion trap was operated in the negative-ion mode with multiple reaction monitoring (MRM) for simultaneous acquisition of MS² traces of up to ten coeluting non-isomeric eicosanoid precursor ions, thus enabling accurate assessment of analytes even under conditions of insufficient chromatographic resolution.

For chromatographic characterization of eicosanoids, the elution of each analyte relative to the retention time (RT) of the non-deuterated IS PGB₁ and SDA as second reference substance was calculated by use of the following equation for the relative retention index (RRI):

$$\text{RRI} = \frac{\text{RT}(\text{SDA}) - \text{RT}(\text{analyte})}{\text{RT}(\text{SDA}) - \text{RT}(\text{PGB}_1)} \quad (1)$$

Mediator identification was performed by use of RRI and both from full UV spectra of the peaks detected on the optical traces and from MS² spectra of the peaks detected on the MS² traces of the analyte precursor ions. MS² analyses of the molecular carboxylate ions of the eicosanoids were performed both offline by DI of single-analyte standards and online by monitoring the MS² spectra of autacoid standards injected on to the interfaced CapLC unit.

Quantitation was performed by IS method using standard mixtures which contained:

1. PGB₁ as a *common* IS when UV *and* MS² or UV detection *alone* was employed, or
2. deuterated eicosanoid standards *and* PGB₁ as IS when MS² detection *alone* was used.

Recoveries were calculated by comparison of the quantities of standards chromatographed after sample extraction with those of standards injected directly in the CapLC–PDAD–ESI–MS² system employing IS method. Measurements were performed for each eicosanoid at six concentrations (*n*=6) and were corrected for endogenous autacoids by subtracting the amounts of eicosanoids found in non-spiked biological matrix from the overall quantities found in the same biological matrix spiked with eicosanoid standards.

Total protein assay

Eicosanoid generation in the lung was expressed as nanograms or picograms of analyte per milligram of lung protein per 240 min. The protein concentration in lung homogenate was determined by an assay based on the Bradford dye-binding procedure [28], with BSA as the protein standard and KHB as the blank. The absorbance change of the Coomassie brilliant blue G-250 dye reagent at 595 nm in response to protein concentration was measured by use of a Biomate 5 spectrophotometer (Thermo Spectronic, Rochester, New York, USA).

Isolated perfused and hypoxically ventilated rabbit lung

As previously described [29], lungs were excised from anaesthetized rabbits, rinsed with KHB for washout of blood, placed in a temperature-equilibrated housing chamber thermostatted at 38.5°C, perfused at 150 mL min⁻¹ and ventilated with a mixture of 5.3% CO₂, 21.0% O₂, balance N₂ (tidal volume, 30 mL; frequency, 30 strokes min⁻¹, positive end-expiratory pressure, 1 cm H₂O). Pulmonary arterial pressure and lung weight were recorded continuously. For hypoxic maneuvers, a gas mixing chamber (KM 60–3/6MESO; Witt, Witten, Germany) was used, this enabled gradual changes in O₂ content from 21% v/v (pO₂ ≈ 160 mmHg, baseline conditions) to 3% v/v (pO₂ ≈ 23 mmHg, hypoxic conditions), 5.3% v/v CO₂, with the balance N₂. After an initial steady-state period of 30 min, time was set to zero and lungs were ventilated with either normoxic or hypoxic gas for 240 min, then homogenized and employed for mediator analysis and protein assay.

Statistics

Analytical data and pulmonary arterial pressure rise (ΔPAP) are expressed as mean ± SEM. Statistical evaluation was performed using one-way analysis of variance (ANOVA). Values of *P*<0.05 for eicosanoid profiles and *P*<0.01 for ΔPAP were considered statistically significant.

Results and discussion

Injection of 8 μL of a standard mixture containing the investigated 44 eicosanoids on to an isocratically eluted capillary column, resulted in chromatographic separation within 50 min followed by dual online PDA (Fig. 2) and MS² (Fig. 3) detection of the eluting analytes.

CapLC–PDAD analysis

The number and position of maxima in the UV spectra of eicosanoids depend on the number and configuration of

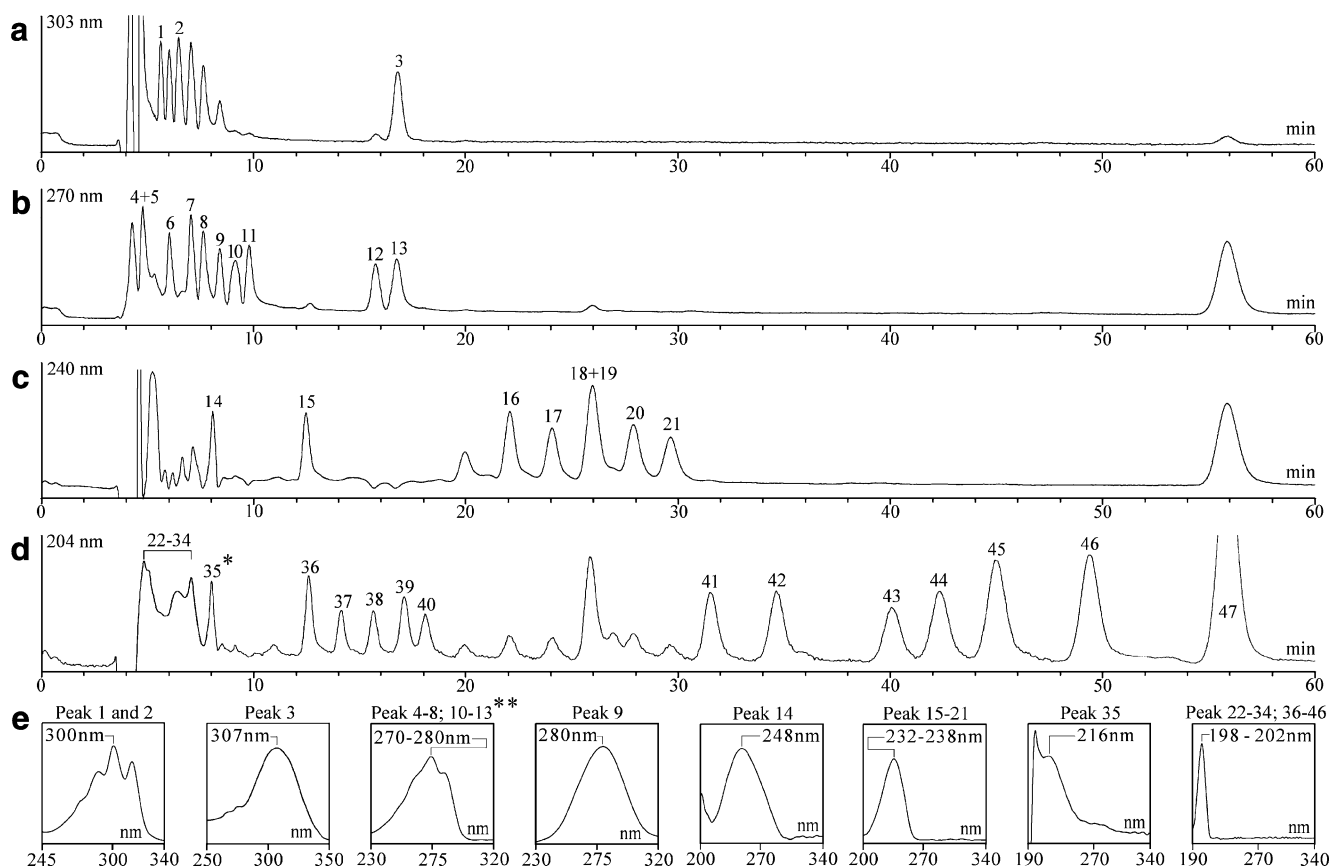


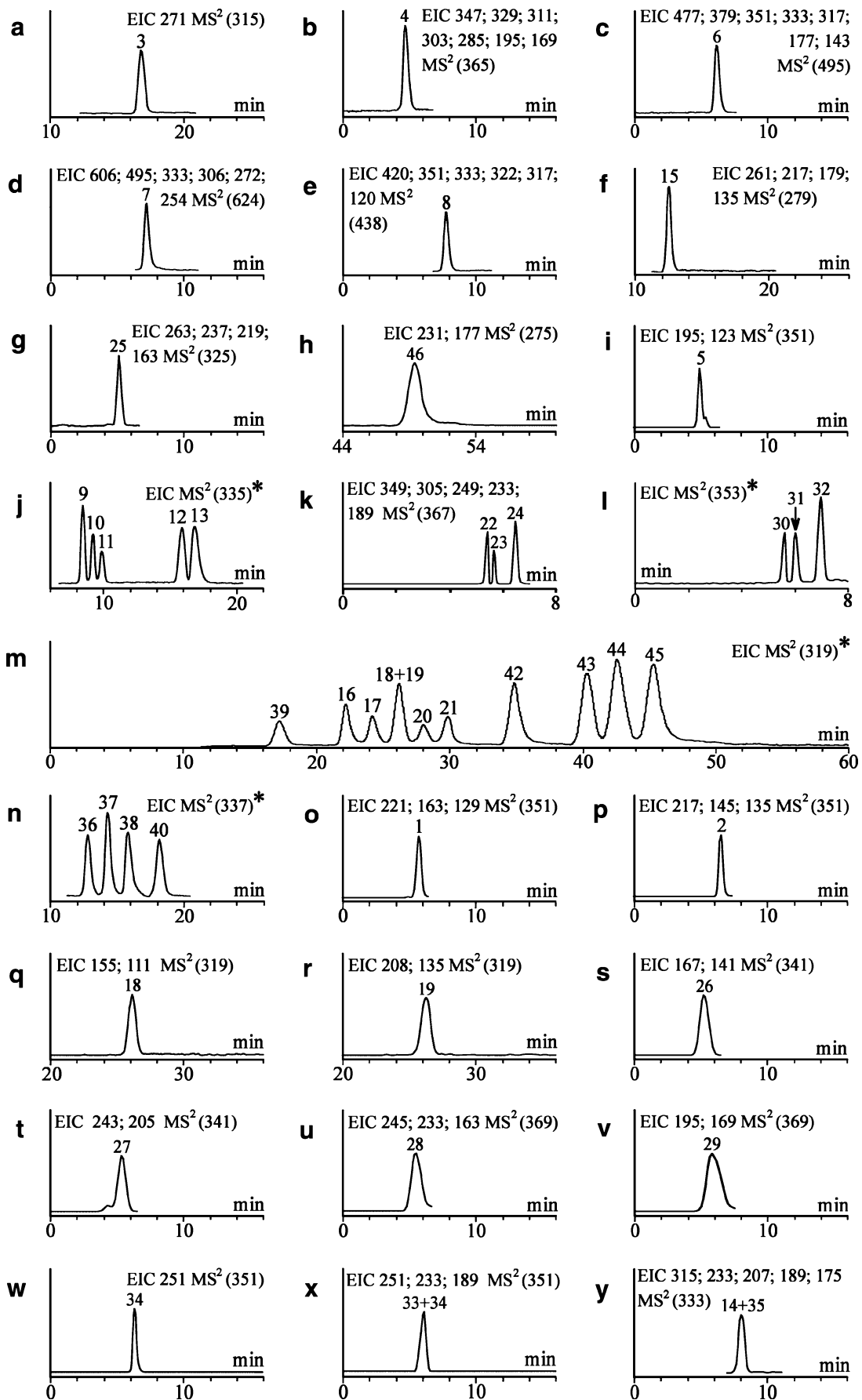
Fig. 2 CapLC-PDAD traces of eicosanoid standards. 8 μ L of a mixture of AA-derived CYP, LOX, and COX metabolites and iPTs were injected on to a capillary column and eluted isocratically. Online PDAD of eluting eicosanoids enabled simultaneous detection at 303 nm (a), 270 nm (b), 240 nm (c), 216 nm (not shown), and 204 nm (d) and identification by spectrum plot on the peak maximum (e), and peak purity control assisted quantitation. Peak designation: 1 = LXB₄; 2 = LXA₄; 3 = 15-deoxy- $\Delta^{12,14}$ -PGJ₂; 4 = 20-COOH-LTB₄; 5 = 20-HO-LTB₄; 6 = LTD₄; 7 = LTC₄; 8 = LTE₄; 9 = PGB₁ = IS; 10 = 6t-LTB₄ + 6t,12e-LTB₄; 11 = LTB₄; 12 = 5(S),6(R)-DiHETE; 13 = 5(S),6(S)-DiHETE; 14 = Δ^{12} -PGJ₂; 15 = 12-HHT; 16 = 15-HETE; 17 = 11-HETE; 18 = 8-HETE; 19 = 12-HETE; 20 = 9-HETE; 21 = 5-HETE; 22 = 19(R)-hydroxy-PGE₂; 23 = 6-keto-PGE₁; 24 = 11-dehydro-TXB₂; 25 =

2,3-dinor-8-*iso*-PGF_{2 α} ; 26 = 2,3-dinor-TXB₂; 27 = 2,3-dinor-6-keto-PGF_{1 α} ; 28 = 6-keto-PGF_{1 α} ; 29 = TXB₂; 30 = 8-*iso*-PGF_{2 α} ; 31 = PGF_{2 α} ; 32 = 13,14-dihydro-15-keto-PGF_{2 α} ; 33 = PGE₂; 34 = PGD₂; 35 = PGJ₂; 36 = 14,15-DHET; 37 = 11,12-DHET; 38 = 8,9-DHET; 39 = 20-HETE; 40 = 5,6-DHET; 41 = 5,6-DHET δ lactone; 42 = 14,15-EET; 43 = 11,12-EET; 44 = 8,9-EET; 45 = 5,6-EET; 46 = SDA; 47 = BHT. *Single asterisk*: PGJ₂ (peak 35) was the sole analyte detected at 216 nm. This optical trace is not displayed for reasons of space. *Double asterisk*: The individual UV spectral maxima were: 270 nm for Peaks 4, 5, 10, and 11 (20-COOH-LTB₄, 20-HO-LTB₄, 6t-LTB₄ + 6t,12e-LTB₄, and LTB₄, respectively), 275 nm for Peaks 12 and 13 (5(S),6(R)-DiHETE and 5(S),6(S)-DiHETE, respectively), and 280 nm for Peaks 6, 7, and 8 (LTD₄, LTC₄, and LTE₄, respectively)

double bonds in their molecules. These spectrophotometric properties were used both for defining the detection wavelengths of analytes with four (303 nm), three (270 nm), two (240 nm and 216 nm) conjugated double bonds and of substances with isolated double bonds (204 nm), and for UV-spectrometric identification of eluting compounds by employing online UV spectra monitored by the PDAD (Fig. 2). The peak numbering employed in Fig. 2 is used throughout this work and was guided by the well-tried practice of consecutive peak integration on the below presented five UV traces (303 nm, 270 nm, 240 nm, 216 nm, and 204 nm) following the elution order within these optical chromatograms rather than the absolute elution order, which cannot be clearly established because of coelution of autacoids belonging to the same or different UV chromatograms.

As specified below, the (partly) coeluting peaks on the same UV traces, for example the peaks 22–34, 4 and 5, and 18 and 19, could be individually assessed by mass-spectrometric detection and were numbered according to their elution order within the individual substance-specific MS² traces.

Quantitation of the eluting eicosanoids was performed by integrating the peak areas on the optical traces at 303 nm (LXs, 15-deoxy- $\Delta^{12,14}$ -PGJ₂) (Fig. 2a), 270 nm (LTs, DiHETEs, PGB₁ = IS) (Fig. 2b), 240 nm (Δ^{12} -PGJ₂, 12-HHT, HETEs) (Fig. 2c), 216 nm (PGJ₂) and 204 nm (19(R)-hydroxy-PGE₂, 6-keto-PGE₁, 11-dehydro-TXB₂, 2,3-dinor-8-*iso*-PGF_{2 α} , 2,3-dinor-TXB₂, 2,3-dinor-6-keto-PGF_{1 α} , 6-keto-PGF_{1 α} , TXB₂, 8-*iso*-PGF_{2 α} , PGF_{2 α} , 13,14-dihydro-15-keto-PGF_{2 α} , PGE₂, PGD₂, 20-HETE, DHETs, EETs,



◀ **Fig. 3** CapLC–ESI–EIC MS² traces of eicosanoid standards. Serial interfacing of the PDAD with an ion-trap mass spectrometer enabled online MS² detection of eluting compounds in the negative-ion mode employing MRM. Mediators were identified and quantified by employing EIC MS² traces defined by summing the intensities of selected substance-specific transitions of the precursor molecular anions. Peak designation is the same as in Fig. 2. *Asterisk*: The complete EIC trace definitions are: (j) EIC 317; 221; 209; 203; 197; 195; 185; 181; 177; 145; 129; 123 MS² (335), (l) EIC 335; 317; 309; 299; 291; 281; 273; 263; 255; 247; 235; 223; 219; 217; 209; 195; 193; 191; 171; 165; 111 MS² (353), (m) EIC 301; 291; 289; 275; 273; 257; 245; 221; 219; 208; 205; 203; 195; 191; 179; 175; 167; 163; 155; 151; 149; 139; 135; 129; 127; 123; 115; 113; 99 MS² (319), (n) EIC 319; 301; 275; 257; 237; 225; 219; 207; 197; 191; 185; 179; 167; 163; 155; 145; 141; 129; 127; 123; 115; 111 MS² (337)

SDA) (Fig. 2d). The optical traces displayed baseline separation for the majority of the eluting compounds, except for peaks 22–34 (22=19(*R*)-hydroxy-PGE₂, 23=6-keto-PGE₁, 24=11-dehydro-TXB₂, 25=2,3-dinor-8-*iso*-PGF_{2α}, 26=2,3-dinor-TXB₂, 27=2,3-dinor-6-keto-PGF_{1α}, 28=6-keto-PGF_{1α}, 29=TXB₂, 30=8-*iso*-PGF_{2α}, 31=PGF_{2α}, 32=13,14-dihydro-15-keto-PGF_{2α}, 33=PGE₂, and 34=PGD₂) at 204 nm, the ω-oxidation products 4 + 5=20-COOH-LTB₄ + 20-HO-LTB₄ at 270 nm and the regioisomers 18 + 19=8-HETE + 12-HETE at 240 nm. Individual assessment of these analytes could be readily performed by detection on substance-specific MS² traces (Fig. 3g,k,l,s,t,u,v,w,x for peaks 22–34, Fig. 3b for 4=20-COOH-LTB₄, Fig. 3i for 5=20-HO-LTB₄, Fig. 3q for 18=8-HETE, and Fig. 3r for 19=12-HETE).

Remarkably, many mediators, for example those with four (LXs, 3=15-deoxy-Δ^{12,14}-PGJ₂), three (LTs, DiHETEs, 9=PGB₁ = IS, 14=Δ¹²-PGJ₂), and two (15=12-HHT, HETEs, 35=PGJ₂) conjugated double bonds, display very characteristic UV spectra with partly multiple maxima at higher, and thus more specific, wavelengths (peaks 1–21 and 35 in Fig. 2e). These UV spectra were particularly suitable for enhancing the reliability of eicosanoid assessment. Thus, identification of several autacoids with “poor” or identical MS² spectra is greatly improved or enabled by online monitoring of UV spectra. For instance, the identity of 3=15-deoxy-Δ^{12,14}-PGJ₂ with only one signal in its MS² spectrum could be confirmed by its characteristic UV spectrum with a maximum at 307 nm (Fig. 2a and e). The individual assessment of the nearly coeluting isomers 14=Δ¹²-PGJ₂ and 35=PGJ₂ with identical MS² spectra was possible only by UV detection, because of their characteristic and distinct UV spectra with maxima at 248 nm and 216 nm, respectively (Fig. 2c,d, and e). Moreover, non-ionic analytes, for example 41=5,6-DHET δ lactone (Fig. 2d and e), the availability of the non-ionic antioxidant 47=BHT (eluting as last peak of the chromatogram and thus not interfering with any eicosanoid peak; Fig. 2d and [electronic supplementary material Fig. S6d](#)) as an effective protective agent at the end of the entire analytical procedure, and possible overloading and thus

malfunction of the high-sensitivity capillary column by large amounts of polar non-ionic matrix interferences could readily be assessed by PDAD but not by ESI–MS².

DI-ESI-MS² and CapLC-ESI-MS² analysis

The mass-spectrometric raw data acquired with the online interfaced ion trap operated in the negative-ion mode using MRM in the MS² stage were used for definition of substance-specific extracted ion chromatograms (EIC) for the precursor molecular anions of the eluting eicosanoids. EIC MS² traces were defined by summing the intensities of several selected substance-specific signals (precursor molecular ion → product/fragment ion transitions) from the MS² spectra of the precursor molecular ions. The EIC trace definitions used in this work were the same as those employed by the Esquire software and by ion trap users [30]. For instance, EIC 420; 351; 333; 322; 317; 120 MS² (438) means that this trace was constructed by summing the intensities of the fragment ions at *m/z* 420, 351, 333, 322, 317, and 120 resulting from MS² transitions, i.e., MS^{*n*} fragmentation stage 2 (*n*=2, MS²), of the molecular ion at *m/z* 438 (corresponding to peak 8=LTE₄; Fig. 3e). The selection of product ions in the EIC MS² trace definition of each eicosanoid was optimized for both maximal EIC signal intensity and substance specificity, thus enabling highly sensitive *and* individual analysis of all mediators, even of coeluting or chromatographically poorly resolved isomeric autacoids in the presence of unknown interfering isomeric compounds from the biological matrix. Figure 3 displays an overview of all EIC MS² traces defined according to the encountered chromatographic situations and grouped as follows:

1. individual assessment of non-isomeric compounds (Fig. 3a,b,c,d,e,f,g,h);
2. individual assessment of isomeric non-coeluting mediators (Fig. 3i,j,k,l,m,n); individual assessment of 18=8-HETE and 19=12-HETE was enabled by the group 3 EIC MS² trace definitions displayed in Fig. 3q and r, respectively;
3. individual assessment of (nearly) coeluting isomers: (Fig. 3o,p,q,r,s,t,u,v,w);
4. assessment of (nearly) coeluting isomeric autacoids together: (Fig. 3x,y).

Quantification of the eluting eicosanoids was performed by integrating the peak areas on the above listed EIC MS² traces. Analyte identity and peak purity were checked by comparing the online monitored compound spectrum with the MS² spectrum of the respective eicosanoid standard obtained offline by DI and/or online by LC–MS² coupling and stored in the MS^{*n*} library module of the Esquire v 5.1 software.

Identity and purity of analyte peaks were triple checked, i.e., chromatographically, by isocratic RRI, and by dual UV-spectrometric and MS² analyses, as demonstrated in Figs. 2, 3, 4 and in [electronic supplementary material](#) Figs. S1, S2, S3, S4).

The molecular carboxylate ions of the eicosanoids (designated *a*) yielded non-characteristic fragments due to neutral loss of CO₂ ($b = a - \text{CO}_2 = a - 44$), H₂O ($a - \text{H}_2\text{O} = a - 18$, $a - 2\text{H}_2\text{O} = a - 36$, $a - 3\text{H}_2\text{O} = a - 54$), loss of both CO₂ and H₂O ($a - \text{CO}_2 - \text{H}_2\text{O} = b - \text{H}_2\text{O} = b - 18$, $a - \text{CO}_2 - 2\text{H}_2\text{O} = b - 2\text{H}_2\text{O} = b - 36$, $a - \text{CO}_2 - 3\text{H}_2\text{O} = b - 3\text{H}_2\text{O} = b - 54$) but also characteristic fragments (designated *c*, *d*, *e*, *f* etc.) because of ring structures or the positions of double bonds and/or functional groups (hydroxyl, epoxide, cysteinyl), as listed in Table 2.

MS² of eicosanoids

The MS² spectra of 12-HHT (*a* at *m/z* 279), the DHETs (*a* at *m/z* 337), and 20-HETE (*a* at *m/z* 319) were similar to those described elsewhere [21, 23, 30]. The spectra of 15=12-HHT, 36=14,15-DHET, 37=11,12-DHET, 38=8,9-DHET, 39=20-HETE, and 40=5,6-DHET are displayed in [electronic supplementary material](#) Figs. S1a,b,c,d,e, and f, respectively. We found that the signal at *m/z* 273 in the MS² spectrum of 20-HETE was presumably formed by loss of carbon dioxide followed by loss of two hydrogen atoms ($d = b - 2\text{H}$) as suggested by the analogous signal at *m/z* 279 ($273 + 6$) generated by MS² analysis of the carboxylate ion (*m/z* 325) of [²H₆]20-HETE with the deuterium atoms at positions 16, 16', 17, 17', 18, and 18'.

The MS² spectra of the LXs LXB₄ (*a* at *m/z* 351) and LXA₄ (*a* at *m/z* 351), the LTs 20-COOH-LTB₄ (*a* at *m/z* 365), 20-HO-LTB₄ (*a* at *m/z* 351), LTD₄ (*a* at *m/z* 495), LTC₄ (*a* at *m/z* 624), LTE₄ (*a* at *m/z* 438), 6-*trans*-LTB₄, 6-*trans*,12-*epi*-LTB₄ and LTB₄, and of 5(*S*),6(*R*)-DiHETE and 5(*S*),6(*S*)-DiHETE (*a* at *m/z* 335, for LTB₄ isomers and DiHETEs) were similar to those reported elsewhere [31–39]. The spectra of 1=LXB₄, 2=LXA₄, 4=20-COOH-LTB₄, 5=20-HO-LTB₄, 6=LTD₄, 7=LTC₄, and 8=LTE₄, 11=LTB₄, are shown in [electronic supplementary material](#) Figs. S2a,b,c,d,e,f, and S3a,b, respectively.

The MS² spectra of the molecular ions (*a* at *m/z* 319) of the HETEs showed signals similar to those described previously [21, 22, 30, 32, 34, 35, 37, 40–43]. The spectra yielded by MS² analysis of 16=15-HETE, 17=11-HETE, 18=8-HETE, 19=12-HETE, and 20=9-HETE, 21=5-HETE are presented in [electronic supplementary material](#) Fig. S3c,d,e,f and Fig. 4a,b, respectively.

Fragmentation of the molecular ions of the EETs (*a* at *m/z* 319) yielded MS² spectra with signals similar to those reported elsewhere [21, 23, 30, 40, 44]. The spectra of 42=

14,15-EET, 43=11,12-EET, 44=8,9-EET, and 45=5,6-EET are displayed in Fig. 4c,d,e, and f, respectively.

The MS² spectra of the prostanoids 6-keto-PGF_{1 α} (*a* at *m/z* 369), 2,3-dinor-6-keto-PGF_{1 α} (*a* at *m/z* 341), 6-keto-PGE₁ (*a* at *m/z* 367), TXB₂ (*a* at *m/z* 369), 11-dehydro-TXB₂ (*a* at *m/z* 367), 2,3-dinor-TXB₂ (*a* at *m/z* 341), PGE₂ (*a* at *m/z* 351), 19(*R*)-hydroxy-PGE₂ (*a* at *m/z* 367), PGD₂ (*a* at *m/z* 351), PGJ₂ (*a* at *m/z* 333), Δ^{12} -PGJ₂ (*a* at *m/z* 333), 15-deoxy- $\Delta^{12,14}$ -PGJ₂ (*a* at *m/z* 315), PGF_{2 α} (*a* at *m/z* 353), 13,14-dihydro-15-keto-PGF_{2 α} (*a* at *m/z* 353), were similar to those described elsewhere [4, 37, 45, 46]. The spectra of 28=6-keto-PGF_{1 α} , 29=TXB₂, 33=PGE₂, 35=PGJ₂, and 34=PGD₂ are illustrated in [electronic supplementary material](#) Figs. S4a,b,d,e, and f, respectively.

Comparative MS² analysis of 33=PGE₂ and 34=PGD₂ was of particular importance for simultaneous and individual assessment of both compounds. Offline MS² analysis of PGD₂ ([electronic supplementary material](#) Fig. S4f) yielded characteristic fragments due to cleavage between C14 and C15 (loss of hexanal) with gain of a hydrogen and charge retention on the carboxyl terminus (*c* at *m/z* 251), prior loss of water from the cyclopentane ring followed by cleavage between C14 and C15 with gain of a hydrogen and charge retention on the carboxyl terminus (*d* at *m/z* 233), and an ion of unknown origin (*e* at *m/z* 189). Comparison of the MS² spectrum of PGE₂ ([electronic supplementary material](#) Fig. S4d) with that of PGD₂ showed no difference with the exception of the fragment ion at *m/z* 251, which is specific for PGD₂ but is lacking in the MS² spectrum of PGE₂. This may be accounted for by facilitation of the prior loss of water from the cyclopentane ring due to the presence of the hydroxyl at C11 in PGE₂, which leads to the formation of a double bond conjugated with the double bond at C13. This conjugation is not achieved for PGD₂, because C11 is occupied by a ketone, thus enhancing the probability of formation of fragment *c* at *m/z* 251 by direct loss of hexanal without prior loss of water. The signal at *m/z* 251 is therefore rather characteristic of PGD₂ and may serve as a basis for individual identification and quantitation of PGD₂ and PGE₂.

PGE₂ was quantified by subtracting the amount of PGD₂ obtained by integration of peak 34 on the EIC 251 MS² (351) trace (Fig. 3w) from the total quantity of PGE₂ and PGD₂ taken together obtained by integration of peaks 33 + 34 on the EIC 251; 233; 189 MS² (351) trace (Fig. 3x). This is possible only in the absence of 1=LXB₄ and 2=LXA₄, because the signals at *m/z* 251, 233, and 189 are also present in the spectra of the nearly coeluting LXs (Table 2, and compare [electronic supplementary material](#) Figs. S4d and f for the spectra of PGE₂ and PGD₂, respectively, with [electronic supplementary material](#) Figs. S2a and b for the MS² spectra of LXB₄ and LXA₄,

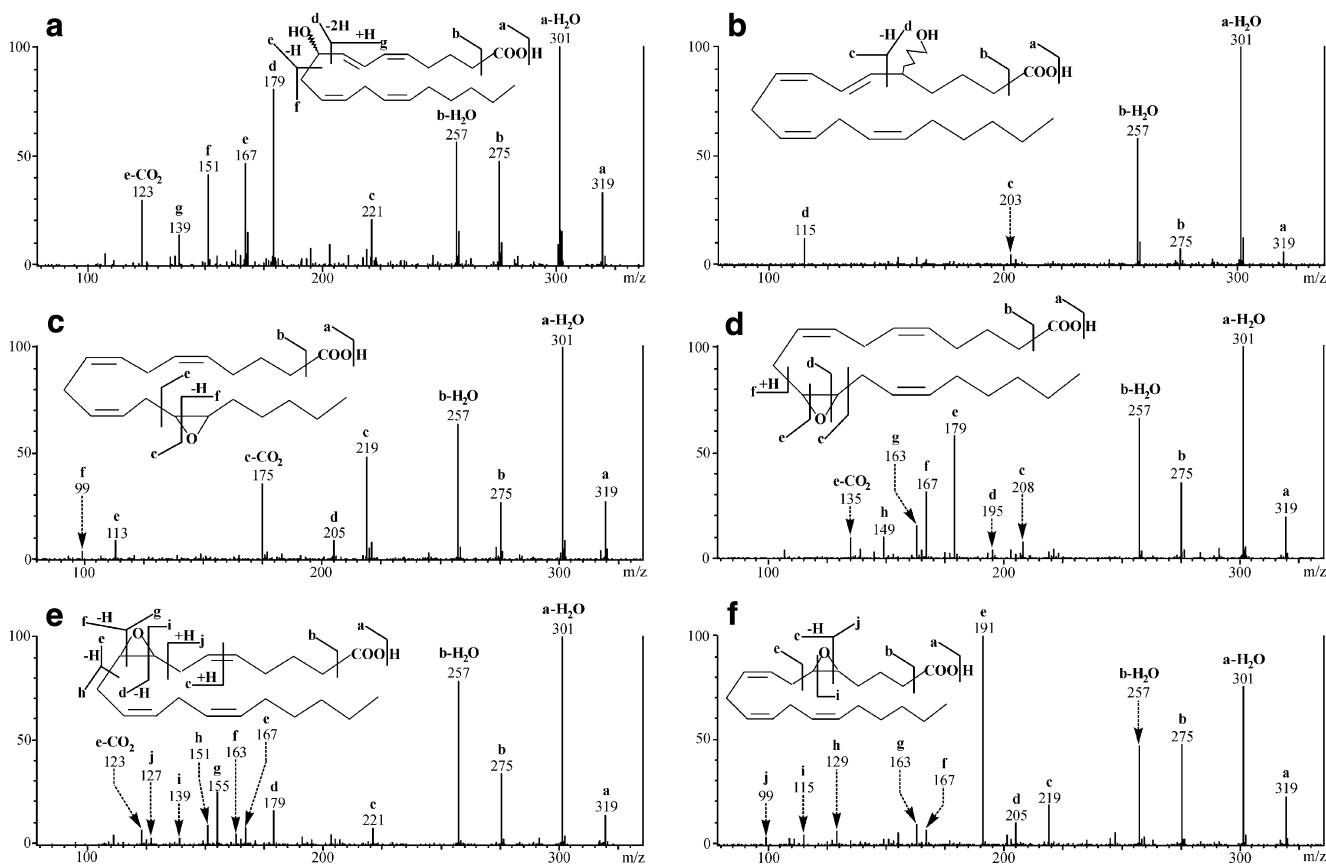


Fig. 4 Exemplary MS² spectra of eicosanoid standards. Online MS² spectra of eluting 20=9-HETE (a), 21=5-HETE (b), 42=14,15-EET (c), 43=11,12-EET (d), 44=8,9-EET (e), and 45=5,6-EET (f).

Eicosanoid numbering is the same as in Fig. 2. Further spectra are provided in the electronic supplementary material

respectively). Conversely, quantitation of LXB₄ and LXA₄ by integration of peak 1 on the EIC 221; 163; 129 MS² (351) trace (Fig. 3o) and peak 2 on the EIC 217; 145; 135 MS² (351) trace (Fig. 3p), respectively, is easily possible, even in the presence of PGE₂ and PGD₂, because the characteristic signals enumerated in the EIC definitions of the two lipoxins are not shared by the two prostaglandins. As the LXs mostly occur, if at all, in very small amounts, the assessment of PGE₂ and PGD₂ is usually unproblematic.

The offline MS² spectrum of 14=Δ¹²-PGJ₂ was identical with that of its nearly coeluting isomer 35=PGJ₂ (electronic supplementary material Fig. S4e; see also Table 2 for MS² signal comparison). Therefore, only MS² identification and quantitation of PGJ₂ and Δ¹²-PGJ₂ taken together (peak 14 + 35=Δ¹²-PGJ₂ + PGJ₂ in Fig. 3y), rather than individually was possible. Fortunately, in contrast to MS² detection, individual identification and quantitation of these two isomers could easily be performed by PDAD because of their characteristic and different UV spectra, as depicted in Fig. 2c–e (see the section CapLC-PDAD analysis, above).

The MS² spectrum (not shown) of 3=15-deoxy-Δ^{12,14}-PGJ₂ displayed no characteristic signals and only one non-characteristic fragment at *m/z* 271 (Table 2). Fortunately, because of its specific UV spectrum (peak 3 in Fig. 2a,e), identification and quantitation reliability could be improved by *additional complementary* PDAD (see the section CapLC-PDAD analysis).

The MS² spectra yielded by fragmentation of the molecular ions of the isoprostanes 30=8-*iso*-PGF_{2α} (*a* at *m/z* 353) (electronic supplementary material Fig. S4c) and its metabolite 25=2,3-dinor-8-*iso*-PGF_{2α} (*a* at *m/z* 325) (not shown) were similar to those reported [4, 45].

Assessment of calibration and recovery

Calibration of the UV and MS signals performed by the IS method, employing PGB₁ as a common IS for all eicosanoids, yielded linear regression functions for all AA metabolites (exemplified for MS² signal calibration in electronic supplementary material Fig. S5).

The described techniques of sample extraction followed by CapLC with dual online PDA and MS² detection were

Table 2 Fragmentation patterns of eicosanoids: m/z values of noncharacteristic fragments H_2O , $b - 2H_2O$, $b - 3H_2O$, and m/z values of characteristic fragment ions resulting from MS^2 analysis of the precursor molecular carboxylate anions (a) due to neutral loss of CO_2 (b = a - CO_2), loss of H_2O (a - H_2O , a - $2H_2O$, a - $3H_2O$), or loss of CO_2 and H_2O (b - and functional groups (hydroxyl, epoxide, cysteinyl))

PN ^a	Compound	Noncharacteristic fragment ions						Characteristic fragment ions										
		a	a - H_2O	a - $2H_2O$	b	a - $3H_2O$	b - $2H_2O$	b - $3H_2O$										
1	LXB ₄	351	333	315	307	289	271	251	233	221	189	163	129	115				
2	LXA ₄	351	333	315	307	289	271	251	235	235	217	215	189	145	135	115		
3	15-deoxy- $\Delta^{12,14}$ -PGJ ₂	315			271													
4	20-COOH-LTB ₄	365	347	329	321	303	285	311	195	169								
5	20-HO-LTB ₄	351	333	315		289	271	195	181	123								
6	LTD ₄	495	477					370	351	333	317	177	143					
7	LTC ₄	624	606					495	333	306	272	254						
8	LTE ₄	438	420					351	333	322	317	120						
9	PGB ₁ = IS	335	317			273		221	209	197	185	177						
10	6 α -LTB ₄	335	317	299		273		195										
10	6 β ,12 α -LTB ₄	335	317	299		273		195										
11	LTB ₄	335	317	299		273	255	203	195	181	177	129	123					
12	5(S),6(R)-DiHETE	335	317	299		273		145										
13	5(S),6(S)-DiHETE	335	317		291	273		145										
14	Δ^{12} -PGJ ₂	333	315			271		233	207	189	175							
15	12-HHT	279	261		235	217		179	163	135	113							
16	15-HETE	319	301		275	257		219	175	113								
17	11-HETE	319	301		275	257		291	195	167	149							
18	8-HETE	319	301		275	257		163	155	127	111							
19	12-HETE	319	301		275	257		208	207	203	179	177	163	153	139	135	107	
20	9-HETE	319	301		275	257		221	179	167	139							
21	5-HETE	319	301		275	257		203	115									
22	19(R)-hydroxy-PGE ₂	367	349	331		305	287	233	189									
23	6-keto-PGE ₁	367	349	331		305	287	249										
24	11-dehydro-TXB ₂	367	349	331		305	287	289	287	261	243	205	191	161	135			
25	2,3-dinor-8-iso-PGF _{2α}	325						263	237	219	163	145	137					
26	2,3-dinor-TXB ₂	341	323	305		305		297	279	261	167	141	123	97				
27	2,3-dinor-6-keto-PGF _{1α}	341	323	305		305		297	279	261	243	235	217	205	187	161	135	
28	6-keto-PGF _{1α}	369	351	333		315		325	307	289	271	263	245	233	215	207	189	163
29	TXB ₂	369	351	333		315		325	307	289	195	177	160	151	125			
30	8-iso-PGF _{2α}	353	335	317		299		309	291	281	273	263	247	235	219	217	209	193
31	PGF _{2α}	353	335	317		299		309	291	281	273	263	247	235	219	217	209	193
32	13,14-dh-15-keto-PGF _{2α} ^b	353	335	317		299		309	291	273	235	223	219	209	195	191	183	165
33	PGE ₂	351	333	315		315	271	233	189									

were: 100 fg for LTs, LXs, PGs, TXs, and iPTs, 300 fg for DHETs, 12-HHT, and DiHETEs, 1 pg for 20-HETE and *cis-trans* conjugated HETEs, and 2 pg for EETs. With 150 μm i.d. columns, the LOQ for MS² detection were a factor of 4 lower. Overall, the LOQ for PDAD were higher than for MS² detection as follows: by a factor of 15 for EETs, DHETs, PGs, TXs, iPTs, and 20-HETE, a factor of 5 for 12-HHT, Δ^{12} -PGJ₂, and *cis-trans* conjugated HETEs, and a factor of 3 for LTs, DiHETEs, LXs, and 15-deoxy- $\Delta^{12,14}$ -PGJ₂. RSD ranged from 6 to 16% ($n=6$).

The actual recovery of each compound was checked with quality control samples freshly prepared prior to SPE of a sample batch from standard stock solutions diluted to the final sample volume with biological matrix and/or KHB, and processed with each set of samples under the same conditions. Moreover, to assess possible non-enzymatic hydrolytic turnover of EETs into the corresponding DHETs during the extraction procedure, quality-control samples containing solely the four EET regioisomers were included in each sample sequence. We found that after storage of dried samples for 24 h at -85°C under an inert N₂ atmosphere the percentages of hydrolyzed EETs (as measured by formation of the corresponding DHET regioisomers and, in the case of 5,6-EET, of 5,6-DHET δ lactone also) were much smaller than the RSD of quantification (6–16%) and thus negligible: 0.77% (14,15-EET), 0.52% (11,12-EET), 0.54% (8,9-EET), 2.31% (5,6-EET). Consequently, it can be assumed that the measured EET and DHET amounts reflect the *in vivo* status quo.

The storage time for biological material and samples was limited to a secure maximum of 24 hours at -85°C with the aim of reducing loss of the thermolabile and reactive EETs (especially the unstable 5,6-EET), which were the focus of this study, to a minimum. These storage conditions were estimated on the basis of maintaining negligibly low hydrolysis rates of EETs to the corresponding DHETs, as shown above. A clear tendency to enhanced hydrolytic turnover was observed after several days of storage. However, we found that within a storage period of a week at -85°C no significant (RSD <16%) decrease of the recoveries of the other eicosanoids occurred. Thus, if the target analytes do not include the EETs, the storage time may be extended to a couple of days.

Features of the developed CapLC–PDAD–ESI–MS² technique

In the past three decades HPLC has developed into a separation technique that provides the highest sensitivity by reducing column i.d. to capillary dimensions [26, 47, 48], thus becoming the method of choice for eicosanoid analysis. The use of PDAD is favored by the fact that, as specified above, many mediators carry strong chromo-

phores, e.g., conjugated double bonds, generating specific UV spectra [18–20]. However, at low analyte concentrations spectrophotometric detection may be difficult, especially for autacoids with weak chromophores, e.g., isolated double bonds. As the assessment of several mediators is enabled and/or greatly improved by PDAD, dual optical *and* mass-spectrometric detection proves to be a reliable *and* sensitive solution for all situations.

The present method employed source-specific SPE with antioxidative protection of analytes and robust isocratic elution of the highly efficient capillary column with a mobile phase of low optical absorption and ionic background noise, followed by online dual PDA *and* MS² detection enabling reliable and highly sensitive assessment of all relevant mediators of the AA cascade and iPTs from complex biological material. The ion-trap technology employed for MS² detection is well suited to lipid mediator analysis [21, 30, 38, 49] and equal in terms of mass accuracy and quantitative sensitivity with triple quadrupole and time-of-flight mass spectrometry [50].

The main characteristics of this technique are:

1. comprehensive *and* rapid analysis of all representative mediators of the AA cascade and iPTs in *one* chromatographic run of 50 min;
2. analytical reliability, accuracy and ruggedness;
3. maximal overall quantitative sensitivity.

Comprehensive and high-throughput CapLC-based analysis of eicosanoids enabled estimation of the *relative* and thus *actual* vasoregulative contribution of the free CYP/SEH-mediated 20-HETE, EETs/DHETs in the context of all the other relevant vasoactive mediators of the AA cascade including the *cis-trans* conjugated HETEs, the LOX-mediated LXs and LTs, the COX-mediated TXs, PGs, and 12-HHT, and the free iPTs as both vasoactive mediators and *in-vivo* markers of ROS-induced oxidative stress/lipid peroxidation by direct comparison of all relevant autacoid generation profiles.

Comprehensive mediator assessment, i.e., analyzing both short-lived primary autacoids and their longer-lived metabolites or degradation products, enables:

1. biochemically accurate mediator profiling by summing the amounts of related metabolites or employing selected representatives. The groups of metabolically related eicosanoids are (generation order; first compound in each group is the precursor): 30=8-*iso*-PGF_{2 α} , 25=2,3-dinor-8-*iso*-PGF_{2 α} ; PGI₂, 28=6-keto-PGF_{1 α} , 27=2,3-dinor-6-keto-PGF_{1 α} , 23=6-keto-PGE₁; TXA₂, 29=TXB₂, 26=2,3-dinor-TXB₂, 24=11-dehydro-TXB₂; the EETs and the corresponding DHETs; 11=LTB₄, 5=20-HO-LTB₄, 4=20-COOH-LTB₄; 7=LTC₄, 6=LTD₄, 8=LTE₄; 33=PGE₂, 22=19(*R*)-hydroxy-PGE₂; 34=PGD₂, 35=PGJ₂, 14= Δ^{12} -PGJ₂, 3=15-deoxy- $\Delta^{12,14}$ -

- PGJ₂; 31=PGF_{2α}, 32=13,14-dihydro-15-keto-PGF_{2α} (see also Fig. 1).
2. quantitation of individual factors of interest, for example 22=19(*R*)-hydroxy-PGE₂, 35=PGJ₂, 14=Δ¹²-PGJ₂, and 3=15-deoxy-Δ^{12,14}-PGJ₂, which have quite specific biological actions, i.e., different physiological functions compared with the respective precursor substance, and can thus not be considered as mere metabolites but rather as physiologically distinct mediators.

In view of the interrelations between COX and CYP [6–8], use of 15 = 12-HHT as an indicator of both TXA₂ synthase [51] and COX [52] activity and as a marker of prostacyclin (PGI₂) generation/PGI₂-dependent relaxation [53] is of special informative importance.

Analytical reliability, accuracy, and ruggedness resulted from:

1. optimal chromatographic resolution of all eicosanoids due to column choice;
2. separation of analytes with reliable selectivity and optimal peak density distribution in a minimal runtime by isocratic elution with a mobile phase adapted to the column used;
3. quantification of eicosanoids by a simple and reliable IS method;
4. robust isocratic elution ensuring, in contrast to gradient elution, maximal reproducibility of retention times and thus, in combination with RRI as selectivity parameter, accurate chromatographic characterization and identification of analytes; followed by
5. dual consecutive online PDA and MS² detection providing a wealth of complementary structural information contained in UV and MS² spectra and thus enabling both maximal analytical reliability for all eicosanoids and simultaneous analysis of a broader array of compounds than with ESI-MS² detection alone.

Maximal overall quantitative sensitivity with LOQ for ESI-MS² detection reaching down to the femtogram range, a key advantage of the presented method, was achieved by:

1. dramatic chromatographic signal gain by use of capillary columns with high peak efficiency instead of large-i.d. columns with low signal yield employed by previous methods;
2. as a result of the inherently low capillary flow rates (0.8–3 μL min⁻¹), virtually complete substance transfer to the mass spectrometer, in contrast to only partial substance transfer at high flow rates (250–1000 μL min⁻¹) typical of large-i.d. columns employed by previous methods;
3. development of a mobile phase with both low ionic background and high optical transparency, due to the use of volatile ionic ingredients at very low concentrations and solvents with low optical absorption, thus increasing the *S/N* ratio for both MS² and PDA detection;

4. increasing the amount of substance on the capillary column by large-volume injection; and
5. increasing the *S/N* ratio by source-specific sample extraction.

It is worthy of note that, because of its high quantitative sensitivity, this CapLC method enabled assessment of *free* EETs, DHETs, 20-HETE, and iPTs, i.e., *active* mediators not esterified into cellular membrane phospholipids, typically occurring at much lower concentrations in biological sources compared with the corresponding autacoids incorporated into phospholipid pools.

Eicosanoid profiling of lungs by global CapLC–PDAD–ESI–MS² analysis

Application of the method to lung homogenate demonstrated that ex-vivo perfused rabbit lungs ventilated under normoxic or hypoxic conditions generated virtually all relevant eicosanoids of the AA cascade including the CYP-mediated free EETs and 20-HETE, the sEH-mediated free DHETs, the LOX-mediated LTs, LXs, and DiHETEs, the COX-mediated TXs, PGs, and 12-HHT, the *cis-trans* conjugated HETEs, and free iPTs, as shown in [electronic supplementary material Fig. S6](#) (optical traces and UV spectra), [Fig. S7](#) (MS² traces), and [Figs. S8 and S9](#) (representative MS² spectra).

A representative profile of eicosanoid formation in hypoxically vs. normoxically ventilated lungs is presented in [Fig. 5](#). The autacoids are grouped according to the three enzymatic generation pathways of the AA cascade—CYP, LOX, and COX. The different eicosanoid classes are represented by selected autacoids as typical examples: EETs/DHETs by their 14,15 and 11,12-regioisomers (42=14,15-EET, 36=14,15-DHET, 43=11,12-EET, 37=11,12-DHET), LTs by 8=LTE₄, *cis-trans* conjugated HETEs by 21=5-HETE, PGs by 31=PGF_{2α}, 33=PGE₂, 34=PGD₂, and PGI₂, and TXs by TXA₂. The iPTs 30=8-*iso*-PGF_{2α} and 25=2,3-dinor-8-*iso*-PGF_{2α} are displayed in the left inset. 1=LXB₄ and 2=LXA₄ were only occasionally found at the detection limit and thus did not disturb assessment of PGE₂ and PGD₂.

Although the CYP-derived EETs are well-known as vasodilatory mediators and putative chemical correlates of EDHF in the cardiovascular compartment [11–14], little is yet known about their vasoregulative role in the lung. However, as previously described [54], these oxiranes were the dominant eicosanoids in the human lung vasculature under conditions of increased pulmonary arterial pressure. Interestingly, application of this technique to isolated perfused lungs revealed substantially enhanced generation of free EETs and their hydration products, the free DHETs, under conditions of hypoxic pulmonary vasoconstriction

(HPV, as assessed by Δ PAP) as compared to normoxic control ventilation conditions (Fig. 5).

The hypothetical *relative* and thus *actual* contribution of the vasoconstrictive and vasodilative eicosanoids to HPV can be assessed by direct comparison of the generation profiles of *all* relevant AA-derived mediators under hypoxic vs. normoxic conditions:

1. Intriguingly, in contrast with the oxiranes, the level of the strong general vasoconstrictor TXA_2 decreased considerably in hypoxic lungs. The levels of the vasoconstrictive free iPTs also decreased, indicating general attenuation of ROS-induced oxidative stress due to decreasing oxygen concentration [3] under hypoxic vs. normoxic ventilation. Moreover, the overall reduced ROS level in hypoxic vs. normoxic ventilated lungs, as assessed by the in-vivo generation of iPTs well matched previous findings obtained by electron spin resonance measurements [55], thus demonstrating

the reliability of both methods. Furthermore, the production of the vasoconstrictive LTE_4 , representative of the LTs, increased, but at very low, negligible concentrations. Consequently, 5-HETE and $\text{PGF}_{2\alpha}$ were the sole vasoconstrictor eicosanoids displaying increasing levels in response to hypoxia and thus contributory to HPV.

2. Remarkably, the levels of the pulmonary vasodilator $39=20\text{-HETE}$ [6] and the potent general vasodilator PGI_2 remained unchanged, while the two vasodilators PGD_2 and PGE_2 displayed opposite generation profiles—increased production of the former, indicating a possible counteraction of HPV, and decreased formation of the latter, suggesting an indirect contribution to HPV. Thus virtually no overall indirect contribution of the vasodilative mediators of the AA cascade to HPV was observed.

The unchanged level of $15=12\text{-HHT}$ clearly correlated with the likewise constant PGI_2 level, thus confirming its

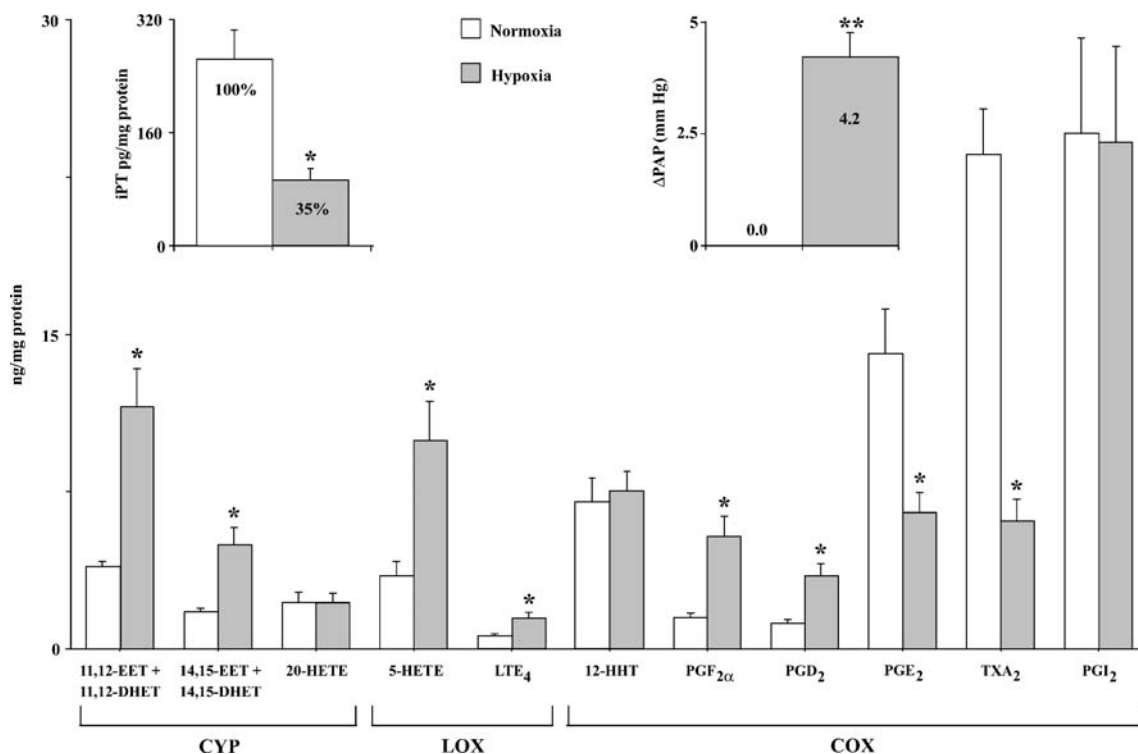


Fig. 5 Global profiling of eicosanoid generation (“eicoprofiling”) in isolated perfused rabbit lungs ventilated for 4 h under hypoxic or normoxic control conditions—exemplary formation profiles of selected mediators from homogenate. The three main enzymatic pathways of the AA cascade are displayed and represented by selected autacoids: the CYP pathway by $39=20\text{-HETE}$, $42=14,15\text{-EET}/36=14,15\text{-DHET}$, and $43=11,12\text{-EET}/37=11,12\text{-DHET}$, the LOX pathway by $21=5\text{-HETE}$ and $8=\text{LTE}_4$, and the COX pathway by $15=12\text{-HHT}$, $31=\text{PGF}_{2\alpha}$, $34=\text{PGD}_2$, $33=\text{PGE}_2$, TXA_2 , and prostacyclin (PGI_2). The unstable prostanoids PGI_2 and TXA_2 were measured as their longer-lived metabolites $28=6\text{-keto-PGF}_{1\alpha}$, $27=2,3\text{-dinoor-6-keto-PGF}_{1\alpha}$, $23=6\text{-keto-PGE}_1$, and $29=\text{TXB}_2$, $26=2,3\text{-dinoor-TXB}_2$, $24=$

11-dehydro-TXB_2 , respectively. The quantitation of $31=\text{PGF}_{2\alpha}$ includes its metabolite $32=13,14\text{-dihydro-15-keto-PGF}_{2\alpha}$. The left inset displays the iPT ($30=8\text{-iso-PGF}_{2\alpha}$ and its metabolite $25=2,3\text{-dinoor-8-iso-PGF}_{2\alpha}$) concentration as an in-vivo indicator of the overall ROS level (displayed in percent on the columns; the normoxic ROS level was set to 100%) in the homogenate of hypoxic and normoxic lungs. Eicosanoid numbering is the same as in Fig. 2. Asterisk: $P < 0.05$ versus control (normoxia). The right inset shows the pulmonary arterial pressure rise (Δ PAP) in hypoxic lungs as a measure of hypoxic pulmonary vasoconstriction (HPV). Double asterisks: $P < 0.01$ versus control (normoxia). Mean \pm SEM; $n=6$

above mentioned role as a prostacyclin inducer and indicator. As a marker of COX activity, 12-HHT also roughly reflects the overall production of TXs and PGs taken together under hypoxic vs. normoxic conditions: increasing amounts of PGF_{2α} and PGD₂ virtually compensated by decreasing amounts of PGE₂ and TXA₂.

Overall, direct comparison of the formation profiles of all relevant vasoactive autacoids has led us to hypothesize that EETs/DHETs may make a substantial contribution to the prolonged HPV response. This presumption correlates well with first reports on vasoconstrictive effects of oxiranes in the pulmonary vasculature [7], on attenuation of HPV by CYP inhibitors [6], and on the hypoxia-induced increase in CYP expression and EET production paralleled by oxirane-elicited HPV, hypertension, and vascular remodeling in mouse lungs [56]. Naturally, the mechanisms of regiospecific and/or enantiospecific EET activity have to be elucidated by further investigations.

Conclusions

The combined method of source-specific SPE followed by isocratic CapLC–PDAD–ESI–MS² enables simultaneous and expeditive, robust, reliable, and highly sensitive analysis of all biological relevant mediators of the AA cascade, and free iPTs, in one chromatographic run of 50 min, thus enabling rapid, comprehensive, and accurate correlations between the biosynthesis at typically very low concentrations and the bioactivity of eicosanoids against the background of varying ROS levels by direct comparison of all autacid generation profiles. To the best of our knowledge, this is the first method suited to accomplishing this task. Application of this approach to homogenates of hypoxically ventilated rabbit lungs revealed at a glance the hypothetical contribution of free CYP/sEH-derived EETs/DHETs to HPV/hypoxic pulmonary hypertension, thus demonstrating the suitability of the method for global “eicoprofiling”.

Acknowledgements We thank Dr Arnd Ingendoh for fruitful discussions. This work was supported by the Deutsche Forschungsgemeinschaft, Project KI 567/1–2 “Vaskuläre Funktionen Cytochrom P450-abgeleiteter Eicosanoide in der pulmonalen Strombahn” and Project GR 1081/4–1 “Synthese und Metabolismus von Eicosanoiden in biologischen Systemen”.

References

- Needleman P, Turk J, Jakschik BA, Morrison AR, Lefkowitz JB (1986) *Annu Rev Biochem* 55:69–102
- Holtzman MJ (1991) *Am Rev Respir Dis* 143:188–203
- Morrow JD, Roberts LJ (2002) *Am J Respir Crit Care Med* 166: S25–30
- Kayganich-Harrison KA, Rose DM, Murphy RC, Morrow JD, Roberts 2nd, LJ (1993) *J Lipid Res* 34:1229–1235
- Fitzpatrick FA, Murphy RC (1989) *Pharmacol Rev* 40:229–241
- Roman RJ (2002) *Physiol Rev* 82:131–185
- Zhu D, Bousamra M 2nd, Zeldin DC, Falck JR, Townsley M, Harder DR, Roman RJ, Jacobs ER (2000) *Am J Physiol Lung Cell Mol Physiol* 278:L335–343
- Michaelis UR, Falck JR, Schmidt R, Busse R, Fleming I (2005) *Arterioscler Thromb Vasc Biol* 25:321–326
- Randriamboavonjy V, Kiss L, Falck JR, Busse R, Fleming I (2005) *Cardiovasc Res* 65:487–494
- Hecker M, Bara AT, Bauersachs J, Busse R (1994) *J Physiol* 481 (Pt 2):407–414
- Campbell WB, Gebremedhin D, Pratt PF, Harder DR (1996) *Circ Res* 78:415–423
- Fisslthaler B, Popp R, Kiss L, Potente M, Harder DR, Fleming I, Busse R (1999) *Nature* 401:493–497
- Busse R, Edwards G, Félétou M, Fleming I, Vanhoutte PM, Weston AH (2002) *Trends Pharmacol Sci* 23:374–380
- Sandow SL (2004) *Clin Exp Pharmacol Physiol* 31:563–570
- Fleming I, Michaelis UR, Bredenkotter D, Fisslthaler B, Dehghani F, Brandes RP, Busse R (2001) *Circ Res* 88:44–51
- Waypa GB, Schumacker PT (2005) *J Appl Physiol* 98:404–414
- Janssen LJ (2004) *Chem Phys Lipids* 128:101–116
- Surette ME, Odeimat A, Palmantier R, Marleau S, Poubelle PE, Borgeat P (1994) *Anal Biochem* 216:392–400
- Yu W, Powell WS (1995) *Anal Biochem* 226:241–251
- Kiss L, Bieniek E, Weissmann N, Schutte H, Sibelius U, Gunther A, Bier J, Mayer K, Henneking K, Padberg W, Grimm H, Seeger W, Grimminger F (1998) *Anal Biochem* 261:16–28
- Bylund J, Ericsson J, Oliw EH (1998) *Anal Biochem* 265:55–68
- Kempen EC, Yang P, Felix E, Madden T, Newman RA (2001) *Anal Biochem* 297:183–190
- Newman JW, Watanabe T, Hammock BD (2002) *J Lipid Res* 43:1563–1578
- Nithipatikom K, DiCamelli RF, Kohler S, Gumina RJ, Falck JR, Campbell WB, Gross GJ (2001) *Anal Biochem* 292:115–124
- Nithipatikom K, Pratt PF, Campbell WB (2000) *Am J Physiol Heart Circ Physiol* 279:H857–H862
- Chervet JP, van Soest REJ, Salzmann JP (1992) *LC GC Intl* 5 (7):33–38
- Héron S, Tchaplal A, Chervet JP (2000) *Chromatographia* 51(7/8):495–499
- Bradford MM (1976) *Anal Biochem* 72:248–254
- Weissmann N, Ebert N, Ahrens M, Ghofrani HA, Schermuly RT, Hanze J, Fink L, Rose F, Conzen J, Seeger W, Grimminger F (2003) *Am J Respir Cell Mol Biol* 29:721–732
- Zelinski V, Borlak J (2005) *Xenobiotica* 35(8):811–823
- Zemski Berry KA, Borgeat P, Gosselin J, Flamand L, Murphy RC (2003) *J Biol Chem* 278:24449–24460
- Wheeler P, Murphy RC (1997) *Anal Biochem* 244:110–115
- Wheeler P, Hankin JA, Bilir B, Guenette D, Murphy RC (1999) *J Pharmacol Exp Ther* 288:326–334
- Sala A, Zarini S, Folco G, Murphy RC, Henson PM (1999) *J Biol Chem* 274:28264–28269
- Griffiths WJ, Yang Y, Sjovald J, Lindgren JA (1996) *Rapid Commun Mass Spectrom* 10:183–196
- Hevko JM, Murphy RC (2001) *J Am Soc Mass Spectrom* 12:763–771
- Margalit A, Duffin KL, Isakson PC (1996) *Anal Biochem* 235:73–81
- Maddox JF, Colgan SP, Clish CB, Petasis NA, Fokin VV, Serhan CN (1998) *FASEB J* 12:487–494
- Fierro IM, Colgan SP, Bernasconi G, Petasis NA, Clish CB, Arita M, Serhan CN (2003) *J Immunol* 170:2688–2694
- Nakamura T, Bratton DL, Murphy RC (1997) *J Mass Spectrom* 32:888–896

41. Kerwin JL, Torvik JJ (1996) *Anal Biochem* 237:56–64
42. Hall LM, Murphy RC (1998) *J Am Soc Mass Spectrom* 9:527–532
43. MacPherson JC, Pavlovich JG, Jacobs RS (1996) *BBA* 1303:127–136
44. Bernstrom K, Kayganich K, Murphy RC (1991) *Anal Biochem* 198:203–211
45. Chiabrando C, Rivalta C, Bagnati R, Valagussa A, Durand T, Guy A, Villa P, Rossi JC, Fanelli R (2002) *J Lipid Res* 43:495–509
46. Zirrolli JA, Davoli E, Bettazzoli L, Gross, M, Murphy RC (1990) *J Am Soc Mass Spectrom* 1:325–335
47. Tomer KB, Moseley MA, Deterding LJ, Parker CE (1995) *Mass Spectrom Rev* 13:431–457
48. Takeuchi T (2005) *Chromatography* 26:7–10
49. Oliw EH, Garscha U, Nilsson T, Cristea M (2006) *Anal Biochem* 354:111–126
50. Jonscher KR, Yates JR III (1997) *Anal Biochem* 244:1–15
51. Hecker M, Haurand M, Ullrich V, Diczfalusy U, Hammarstrom S (1987) *Arch Biochem Biophys* 254:124–135
52. Sweeney FJ, Pereira MJ, Eskra JD, Carty TJ (1987) *Prostaglandins Leukot Med* 26:171–177
53. Sadowitz PD, Setty BN, Stuart M (1987) *Prostaglandins* 34:749–763
54. Kiss L, Schütte H, Mayer K, Grimm H, Padberg W, Seeger W, Grimminger F (2000) *Am J Respir Crit Care Med* 161:1917–1923
55. Weissmann N, Kuzkaya N, Fuchs B, Tiyerili V, Schafer RU, Schutte H, Ghofrani HA, Schermuly RT, Schudt C, Sydykov A, Egemnazarow B, Seeger W, Grimminger F (2005) *Respir Res* 6:86. DOI 10.1186/1465-9921-6-86
56. Pokreisz P, Fleming I, Kiss L, Barbosa-Sicard E, Fisslthaler B, Falck JR, Hammock BD, Kim IH, Szelid Z, Vermeersch P, Gillijns H, Pellens M, Grimminger F, Zonneveld AJ, Collen D, Busse R, Janssens S (2006) *Hypertension* 47:762–770